International Journal of Power Electronics and Drive System (IJPEDS)
Vol. 5, No. 3, February 2015, pp. 315~325
ISSN: 2088-8694

Speed Sensorless Vector Control of Induction Motor Drive with PI and Fuzzy Controller

R. Gunabalan*, V. Subbiah**
* Departement of Electrical and Electronics Engineering, Dr. Sivanthi Aditanar College of Engineering, Tiruchendur
** Departement of Electrical and Electronics Engineering, PSG College of Technology, Coimbatore

Article Info

Article history:

Received Sep 12, 2014
Revised Dec 25, 2014
Accepted Jan 8, 2015

Keyword:

Fuzzy controller
Induction motor
Natural observer
Sensorless control
Simulation

ABSTRACT

This paper directed the speed-sensorless vector control of induction motor drive with PI and fuzzy controllers. Natural observer with fourth order state space model is employed to estimate the speed and rotor fluxes of the induction motor. The formation of the natural observer is similar to and as well as its attribute is identical to the induction motor. Load torque adaptation is provided to estimate the torque and rotor speed is estimated from the load torque, rotor fluxes and stator currents. There is no direct feedback in natural observer and also observer gain matrix is absent. Both the induction motor and the observer are characterized by state space model. Simple fuzzy logic controller and conventional PI controllers are used to control the speed of the induction motor in closed loop. MATLAB simulations are made with PI and fuzzy controllers and the performance of fuzzy controller is better than PI controller in view of torque ripples. The simulation results are obtained for various running conditions to exhibit the suitability of this method for sensorless vector control. Experimental results are provided for natual observer based sensorless vector control with conventional PI controller.

Corresponding Author:

R. Gunabalan,
Departement of Electrical and Electronics Engineering,
Chandy College of Engineering, Thoothukudi 628005
Anna University, Chennai, TamilNadu, INDIA.
Email: gunabalanr@yahoo.co.in

1. INTRODUCTION

Induction motors are preferred for most of the industry applications because of the limitations of commutation and rotor speed in DC drives. The induction motor is in fact 'brushless' and can operate with simple control methods not requiring a shaft position transducer. With no shaft position feedback, the motor remains stable only as long as the load torque does not exceed the breakdown torque. At low speeds it is possible for oscillatory instabilities to develop. To overcome these limitations 'field-oriented' or 'vector' control has been developed in which the phase and magnitude of the stator currents are regulated so as to maintain the optimum angle between stator mmf and rotor flux. This control is based on transforming a three phase time and frequency dependent system into a two co-ordinate (d and q axes) time invariant system. These projections lead to a structure similar to that of a separately excited DC motor control. Field orientation, however, requires either a shaft position encoder or an in-built control model whose parameters are specific to the motor.

Generally, two types of field oriented control schemes are available. 1. Direct field oriented control 2. Indirect field oriented control. In the direct scheme, the instantaneous position of rotor flux (θ_e) has to be measured using flux sensors. This adds to the cost and complexity of the drive system. In the indirect scheme, a model of the induction motor is required to calculate the reference angular slip frequency that has to be added to the measured rotor speed. The sum is integrated to calculate the instantaneous position of the

rotor flux. Rotor time constant (L_r/R_r) is used to calculate the slip frequency and is sensitive to temperature and flux level. To avoid these complications, different algorithms are projected, to estimate both the rotor flux vector and/or rotor shaft speed. The induction motor drives without mechanical speed sensors have the attractions of low cost, high reliability, smaller in size and lack of additional wiring for sensors or devices mounted on the shaft. Nowadays, a number of estimation techniques are available for speed and flux calculation. The standard speed estimators are Extended Kalman Filter (EKF) [1]–[6], Luenberger observer [7]–[9] and Model Reference Adaptive System (MRAS) [10]. The initial selection of noise covariance matrices is not easy in EKF and subsequently the algorithm is complicated. The selection of the observer gain constant is difficult in Luenberger observer. The number of inputs to the estimators mentioned above is different to the number of inputs to the induction motor since they utilize output feedback. To overcome the difficulties of the above estimators, natural observer proposed in [11] is used in this paper. In natural observer, the dynamic behavior is exactly the same as the motor and there is no external feedback. The load torque adaptation is used to estimate the load torque from the active power error. Fifth order state space model was used in [11] whereas fourth order induction motor model is used in this paper to reduce the computational burden and the equations are similar to Luenberger observer.

Recent developments in the application of control theory are such that the conventional techniques for the design of controllers are being replaced by artificial intelligence based controllers. The main purpose of using artificial intelligence based controllers is to reduce the tuning efforts associated with the conventional PI controllers and also to obtain the improved responses. PID controllers are commonly intended for linear systems and they provide a preferable cost/benefit ratio [12]. However, the presence of nonlinear effects limits their performances.

Fuzzy logic controllers (FLC's) have the following advantages over the conventional controllers [13]: they are cheaper to develop, they cover a wider range of operating conditions, and they are more readily customizable in natural language terms. Application of PI-type fuzzy controller increases the quality factor. In contrast with traditional linear and nonlinear control theory, a FLC is not based on a mathematical model and is widely used to solve problems under uncertain and vague environments, with high nonlinearities.

In this paper, natural observer with reduced order state space model is proposed to estimate the speed of the induction motor and fuzzy controller is employed instead of conventional PI controller for speed control. Mean value of the rotor flux is maintained constant by employing PI controller in the rotor flux feedback path. Simulations are performed for different running conditions to study the performance of fuzzy controller over PI controller. Experimental results are provided with PI controller to validate the proposed method.

2. NATURAL OBSERVER

The arrangements and the characteristics of the natural observer are similar to the induction motor for the specified input voltage and load torque condition. The major difference between the natural observer and the conventional observer is that feedback is employed only in the adaptation algorithm and no direct feedback. So, the convergence rate of the natural observer is faster than that of the motor in reaching the steady state behaviour. To estimate the rotor speed, fourth order induction motor model in stator flux oriented reference frame is used in this paper, whereas fifth order state space model is used in [11]. The dq-axes stator currents and rotor fluxes are considered as state variables. The state space representation of the three-phase induction motor is as follows:

$$\frac{dX}{dt} = AX + BV_s \quad (1)$$

$$Y = CX \quad (2)$$

Where,

$$A = \begin{bmatrix} \frac{-\left(R_s + R_r\left(\frac{L_m}{L_r}\right)^2\right)}{\sigma L_s} & 0 & \frac{L_m}{\sigma L_s L_r \tau_r} & \frac{\omega_r L_m}{\sigma L_s L_r} \\ 0 & \frac{-\left(R_s + R_r\left(\frac{L_m}{L_r}\right)^2\right)}{\sigma L_s} & \frac{-\omega_r L_m}{\sigma L_s L_r} & \frac{L_m}{\sigma L_s L_r \tau_r} \\ \frac{L_m}{\tau_r} & 0 & \frac{-1}{\tau_r} & -\omega_r \\ 0 & \frac{L_m}{\tau_r} & \omega_r & \frac{-1}{\tau_r} \end{bmatrix}$$

$$B = \begin{bmatrix} \frac{1}{\sigma L_s} & 0 \\ 0 & \frac{1}{\sigma L_s} \\ 0 & 0 \\ 0 & 0 \end{bmatrix} C = \begin{bmatrix} 1 & 0 & 0 & 0 \\ 0 & 1 & 0 & 0 \end{bmatrix}$$

$\sigma = 1 - \frac{L_m^2}{L_s L_r}$ - leakage coefficient

$X = \left[i_{ds}^s \quad i_{qs}^s \quad \varphi_{dr}^s \quad \varphi_{qr}^s \right]^T$

$Y = [i_{ds}^s \quad i_{qs}^s] = i_s$

$V_s = [V_{ds}^s \quad V_{qs}^s]^T$

L_s, L_r – stator and rotor self inductance respectively (H)

L_m- mutual inductance (H)

τ_r-rotor time constant $= \frac{L_r}{R_r}$

ω_r -motor angular velocity (rad/s)

Figure 1 shows the structure of the natural observer and the system described by Equation (1) and Equation (2) are exactly the same form of the induction motor model and no external feedback [11]. Estimation of the stator currents and the rotor fluxes can be written by the following equations:

$$\frac{d\hat{X}}{dt} = \hat{A}\hat{X} + BV_s \tag{3}$$

$$\hat{Y} = C\hat{X} \tag{4}$$

$\hat{X} = \left[\hat{i}_{ds}^s \quad \hat{i}_{qs}^s \quad \hat{\varphi}_{dr}^s \quad \hat{\varphi}_{qr}^s \right]^T$

$\hat{Y} = [\hat{i}_{ds}^s \quad \hat{i}_{qs}^s]^T = \hat{i}_s$

Where, "^" represents the estimated quantities.

The load torque is estimated from the active power error by the following equation [11]:

$$\widehat{T_L} = K_P e_P + K_I \int e_P \, dt \tag{5}$$

$$e_P = V_{ds}^s (\hat{i}_{ds}^e - i_{ds}^e) + V_{qs}^s (\hat{i}_{qs}^e - i_{qs}^e) \tag{6}$$

Rotor speed is estimated from the estimated stator current, rotor flux and the estimated load torque and it is represented as follows [14]:

$$\dot{\widehat{\omega_r}} = \left(\frac{3}{2}\right)\left(\frac{n_p}{J}\right)\left(\frac{L_m}{L_r}\right)\left[\hat{\varphi}_{dr}^s \hat{i}_{qs}^s - \hat{\varphi}_{qr}^s \hat{i}_{ds}^s\right] - \frac{\widehat{T_L}}{J} \tag{7}$$

Where n_p is the no. of pole pairs and J is of inertia of motor load system (kg.m^2).

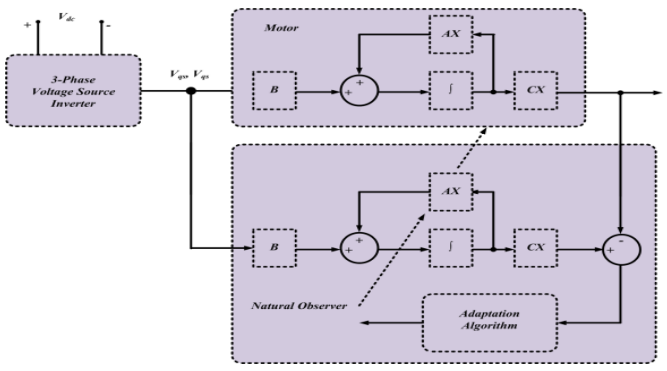

Figure 1. Structure of a natural observer

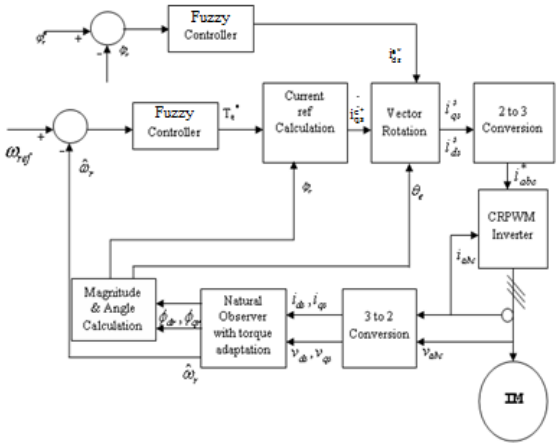

Figure 2. Closed loop sensorless speed control of induction motor drive with fuzzy controller

The closed loop structure of the natural observer is shown in Figure 2. The main components are: natural observer with adaptive load torque estimation, calculation blocks of reference current values, PI/fuzzy controllers and current regulated pulse width modulated (CRPWM) voltage source inverter. The space vector model of the induction motor is used to derive the equations for i_{ds}^{e*} and i_{qs}^{e*} and are as follows [14]:

$$V_{ds}^{e} = i_{ds}^{e}R_s + p\varphi_{ds}^{e} + j\omega_e\varphi_{ds}^{e} \quad (8)$$

$$V_{qs}^{e} = i_{qs}^{e}R_s + p\varphi_{qs}^{e} + j\omega_e\varphi_{qs}^{e} \quad (9)$$

$$0 = i_{dr}^{e}R_r + p\varphi_{dr}^{e} + j(\omega_e - \omega_r)\varphi_{dr}^{e} \quad (10)$$

$$0 = i_{qr}^{e}R_r + p\varphi_{qr}^{e} + j(\omega_e - \omega_r)\varphi_{qr}^{e} \quad (11)$$

$$\varphi_{ds}^{e} = L_s i_{ds}^{e} + L_m i_{dr}^{e} \quad (12)$$

$$\varphi_{qs}^{e} = L_s i_{qs}^{e} + L_m i_{qr}^{e} \quad (13)$$

$$\varphi_{dr}^{e} = L_r i_{dr}^{e} + L_m i_{ds}^{e} \quad (14)$$

$$\varphi_{qr}^{e} = L_r i_{qr}^{e} + L_m i_{qs}^{e} \quad (15)$$

$$T_e = \frac{3}{2}\frac{P}{2}\left(\frac{L_m}{L_r}\right)\left(\varphi_r^{e} \times i_s^{e}\right) \quad (16)$$

$$T_e = \frac{3}{2}\frac{P}{2}\left(\frac{L_m}{L_r}\right)\left(\varphi_{dr}^{e} i_{qs}^{e} - \varphi_{qr}^{e} i_{ds}^{e}\right) \quad (17)$$

From Equation (10):

$$i_{dr}^{e} = \frac{-p\varphi_{dr}^{e} - j(\omega_e - \omega_r)\varphi_{dr}^{e}}{R_r} \quad (18)$$

By substituting in Equation (14):

$$\varphi_{dr}^{e} = L_r\frac{-p\varphi_{dr}^{e} - j(\omega_e - \omega_r)\varphi_{dr}^{e}}{R_r} + L_m i_{ds}^{e} \quad (19)$$

Further after simplification,

$$p\varphi_{dr}^{e} + \{S_r + j(\omega_e - \omega_r)\}\varphi_{dr}^{e} = L_m S_r i_{ds}^{e} \quad (20)$$

Similarly,

$$p\varphi_{qr}^{e} + \{S_r + j(\omega_e - \omega_r)\}\varphi_{qr}^{e} = L_m S_r i_{qs}^{e} \quad (21)$$

From Equation (20) and Equation (21), the general equation is represented as:

$$p\varphi_{r}^{e} + \{S_r + j(\omega_e - \omega_r)\}\varphi_{r}^{e} = Ui_{s}^{e} \quad (22)$$

where, $U = S_r L_m$; $S_r = \frac{R_r}{L_r}$

$$p\left(\varphi_{dr}^{e} + j\varphi_{qr}^{e}\right) + \{S_r + j(\omega_e - \omega_r)\}\left(\varphi_{dr}^{e} + j\varphi_{qr}^{e}\right) = U\left(i_{ds}^{e} + ji_{qs}^{e}\right) \quad (23)$$

Separating real and imaginary parts,

$$p\varphi_{dr}^{e} + S_r\varphi_{dr}^{e} - \omega_e\varphi_{qr}^{e} + \omega_r\varphi_{qr}^{e} = Ui_{ds}^{e} \quad (24)$$

For constant flux operation, $p\varphi_{dr}^{e} = 0$ and $\varphi_{qr}^{e} = 0$ and i_{ds}^{e} is calculated as follows:

$$S_r\varphi_{dr}^{e*} = Ui_{ds}^{*} = S_r L_m i_{ds}^{e*} \quad (25)$$

$$i_{ds}^{e*} = \frac{i_{ds}^{e*}}{L_m} \quad (26)$$

Torque developed in an induction motor

$$T_e = \left(\frac{P}{2}\right)\frac{L_m}{L_r}\left(\varphi_r \times i_s\right) \quad (27)$$

$$T_e = \left(\frac{P}{2}\right)\frac{L_m}{L_r}\left(\varphi_{dr}^{e} i_{qs}^{e} - \varphi_{qr}^{e} i_{ds}^{e}\right) \quad (28)$$

i_{qs}^{e*} controls the average torque developed,

$$i_{qs}^{e*} = \frac{L_r}{\frac{P}{2}L_m\varphi_{dr}^{*}}T^{*} \quad (29)$$

$$i_{qs}^{e*} = \frac{L_r}{n_p L_m\varphi_{dr}^{*}}T^{*} \text{ where } n_p \text{ is the pole pair} \quad (30)$$

i_{ds}^{e*} is generated by comparing the actual flux with the set reference flux and the error is given to the PI controller which gives the desired value of i_{ds}^{e*}. In addition, it maintains the mean value of rotor flux as constant. The reference currents are transformed into stationary reference frame by rotor angle θ_e. The two phase dq-axes stator currents are transformed into three phase reference current by 2 to 3 conversion blocks (inverse Clarke's transformation).

3. FUZZY LOGIC CONTROLLER

Fuzzy logic can be described simply as "computing with words rather than numbers''; "control with sentences rather than equations''. A fuzzy controller includes empirical rules and is useful in operator controlled plants. Fuzzy control is preferred where robust control is desired, particularly with plant parameter variations and load disturbance effects. There is no design procedure in fuzzy control such as root-locus design, frequency response design, pole placement design or stability margins, because the rules are often nonlinear. Fuzzy controllers are being used in various control schemes. In this work, direct control is used, where the fuzzy controller is in the forward path in a feedback control system. The process output is compared with a reference, and if there is a deviation, the controller takes action according to the control strategy. Triangular memberfunctions were used in most of the literatures [15]-[16] whereas Gaussian membership functions are selected in this paper as they are smooth and nonzero at all points. The control

signals are error (E) and change in error (CE). The fuzzy controller fuzzifies the input signals and generates the control signal through the evaluation of control rules and defuzzification. All the input and output signals use Gaussian membership functions. Mamdani type inference method and mean of maximum (This method disregards the shape of the fuzzy set, but the computational complexity is relatively good) defuzzification method are used. The linguistic membership functions are negative large (NL), negative small (NS), zero (Z), positive small (PS) and positive large (PL).

The rule matrix for fuzzy control is given in Table 1. As example, the control rules for E and CE are:

1. If E is Z and CE is Z then control signal is Z
2. If E is PS and CE is Z then control signal is PS
3. If E is Z and CE is NS then control signal is NS

The membership functions for the input variable error, change in error and the control signal are shown in Figure 3.

Table 1. Rule table for fuzzy control

CE / E	NL	NS	Z	PS	PL
NL	NL	NL	NS	NS	Z
NS	NL	NS	NS	Z	PS
Z	NS	NS	Z	PS	PS
PS	NS	Z	PS	PS	PL
PL	Z	PS	PS	PL	PL

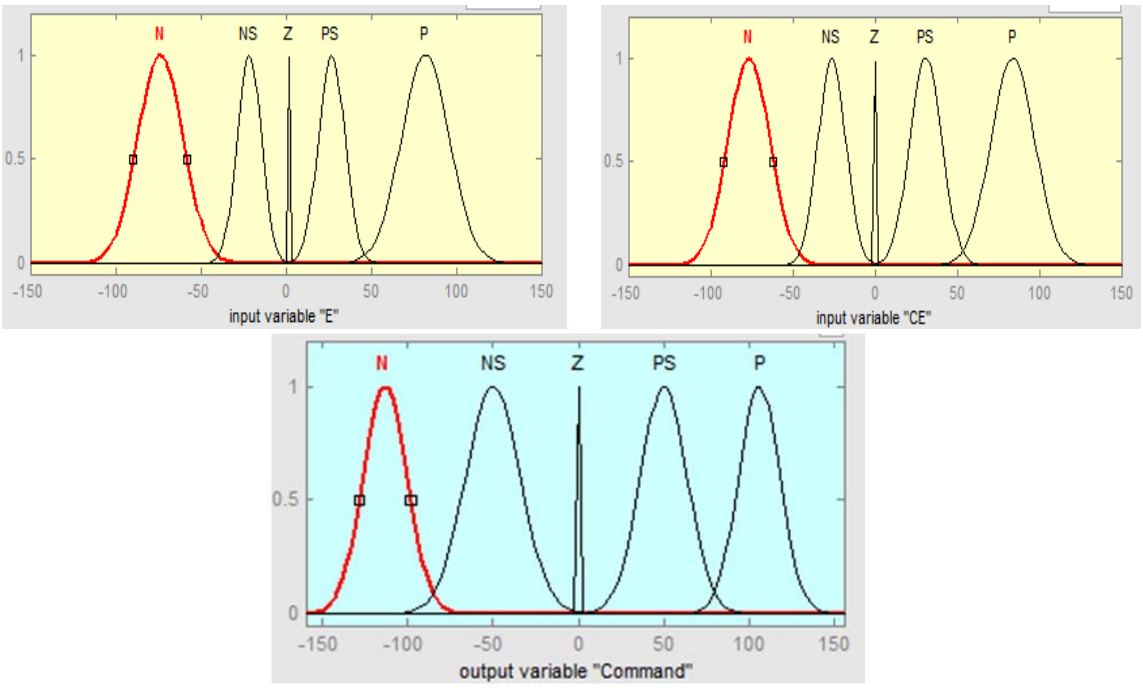

Figure 3. Fuzzy membership functions

4. SIMULATION RESULTS AND DISCUSSIONS

Simulations are done in MATLAB simulink atmosphere. The simulation blocks of sensorless vector control are constructed in MATLAB using power system blocksets and simulink libraries. Natural observer is used to estimate the speed, rotor fluxes and stator currents. Conventional PI controller and fuzzy controller are investigated. The simulation results are presented for different running conditions. The ratings and the parameters of the induction motor are given in Table 2. Direct field oriented sensorless vector control scheme is used and the rotor angle is determined from the estimated rotor fluxes. The torque adaptation gains are

K_p=0.08, K_I=0.2. Figure 4 and Figure 5 show the simulation diagram of sensorless vector control of induction motor drive with PI controller and fuzzy controller respectively. The induction motor and the natural observer are built with state space model and are constructed by MATLAB functions. In addition, various simple blocks available in simulink are used to construct the entire system. PI controller is constructed using PID block available in simulink libraries. The simulation blocks of fuzzy controller are constructed in MATLAB using fuzzy toolbox. Fuzzy controller is framed with 5 linguistic variables to generate the required torque reference signal from the speed error. It also reduces the computational burden in real time.

The simulation results of speed sensorless vector control of induction motor drive with PI controller and fuzzy speed controller for different running conditions are shown in Figure 6. The motor is at no load at the time of starting. The speed command is set at 500 rpm. At t = 1.5s, a step speed command is given to increase the speed from 500 rpm to 750 rpm. At t=3s, a load of 1.5 Nm is applied. It is observed from the Figure 6(a) that the estimated speed follows the actual speed. At steady state, the difference between estimated and actual speed is zero. During starting as well as change in speed, the peak magnitude of the actual torque is less in fuzzy controller than PI controller and also the transient torque at the time of change in speed is very high in PI controller and it is suppressed in fuzzy controller. The estimated and actual torque responses are shown in Figure 6(b). Simulations are also investigated at a speed of 1000 rpm and the results are described in Figure 7.

Table 2. Ratings and parameters of induction motor

Parameters	Ratings
Output	745.6 W
Poles	4
Speed	1415 rpm
Voltage	415 V
Current	1.8 A
R_s	19.355 Ω
R_r	8.43 Ω
L_s	0.715 H
L_r	0.715 H
L_m	0.689 H
f	50 Hz

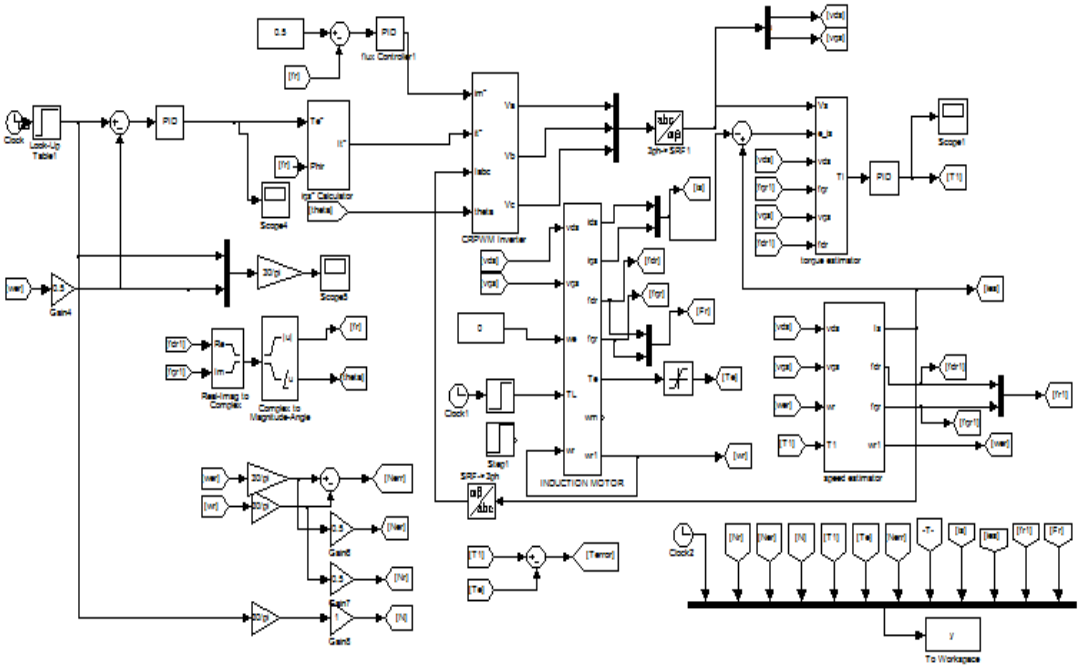

Figure 4. Simulation diagram of speed sensorless vector control of induction motor drive with PI controller

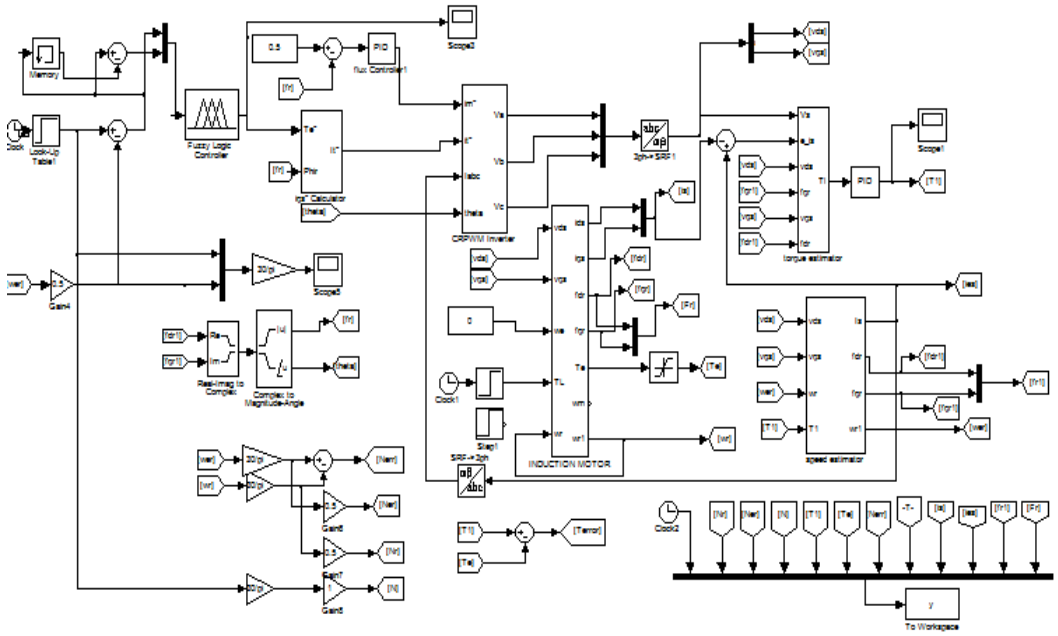

Figure 5. Simulation diagram of speed sensorless vector control of induction motor drive with fuzzy controller

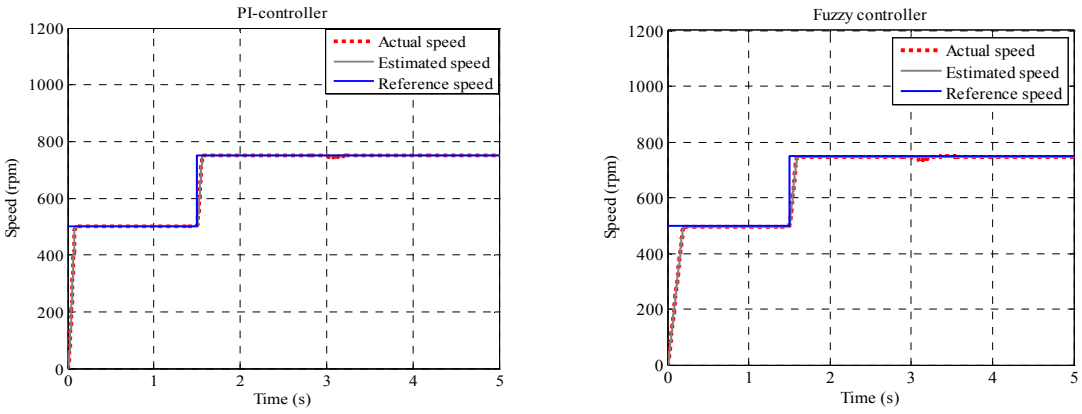

(a) Estimated and actual speed response

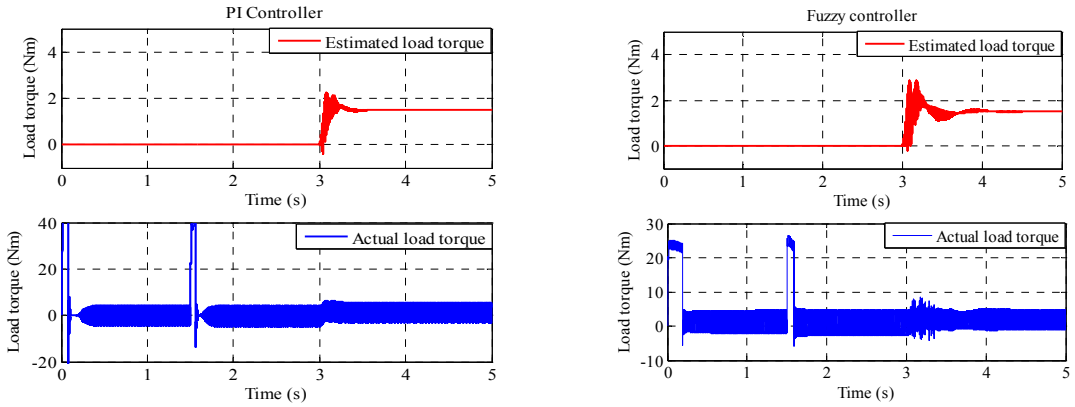

(b) Estimated and actual torque response

Figure 6. Simulation waveform for a speed of 500 rpm and 750 rpm with 1.5 Nm load

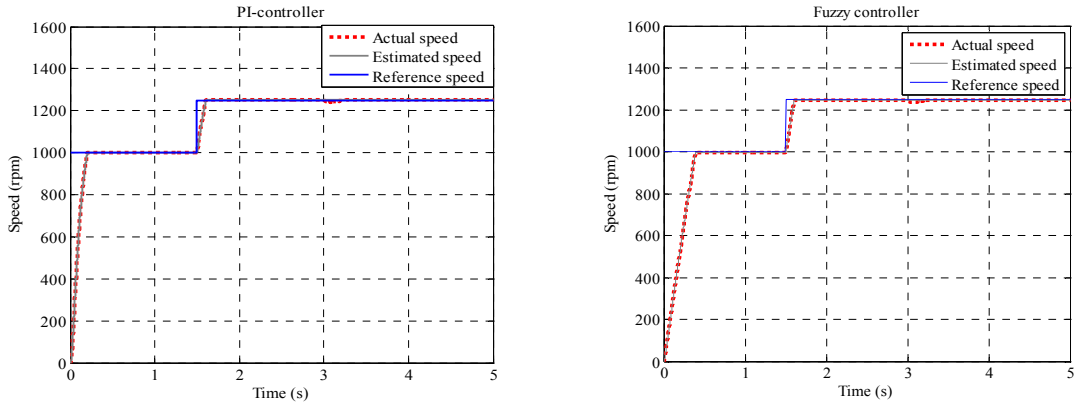

(a) Estimated and actual speed response

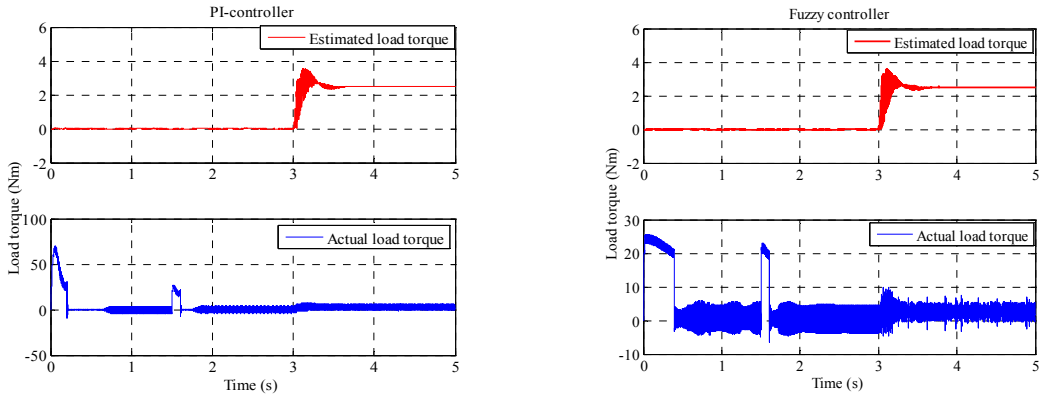

(b) Estimated and actual torque response

Figure 7. Simulation waveform for a speed of 1000 rpm and 1250 rpm with 2.5 Nm load

5. HARDWARE RESULTS AND DISCUSSIONS

Three-phase squirrel cage induction motor of 0.746 kW (1HP) is used for the experimental set up. Brake drum arrangements are provided for mechanical loading. The central processor unit is the TMS320F2812 DSP processor and it executes all the mathematical calculations. Various simulink blocks like natural observer and PI controllers are built in VISSIM. TMS320F2812 DSP processor supporting blocks are available in VISSIM. In VISSIM, the simulation blocks are converted into C- codes using the target support for TMS320F2812 and compiled using code composer studio internally and the output file is downloaded into the DSP processor through J-tag emulator. Three numbers of LEM current sensors and voltage sensors are used to measure the phase currents and terminal voltages of the induction motor respectively. The measured analog currents and voltages are converted into digital by on chip ADC with 12 bit resolution. The feedback signals are linked to DSP processor using 26 pin header and the processor estimates the stator current, rotor flux, load torque and speed. The processor also generates the required PWM pulses to enable the three phase IGBT inverter switches in the Intelligent Power Module (IPM). Highly effective over-current and short-circuit protection is realized through the use of advanced current sense IGBT chips that allow continuous monitoring of power device current. System reliability is further enhanced by the IPM's integrated over temperature and under voltage lock out protection.

The experimental results for a step change in speed of 1000 rpm to 1250 rpm for a load of 2.5 Nm are shown in Figure 8. The actual speed of the motor is measured by proximity sensor. The estimated and actual speed waveforms for step increase and decrease in speed are depicted in Figure 8(a) and Figure 8(b) respectively. It is observed that the estimated speed follows the actual speed and matches with the simulation waveform. The estimated speed response with respect to the reference speed of 1250 rpm (500 rpm/div) is presented in Figure 8(c) for a load of 2.5 Nm (1 Nm/div). It is inferred that drop in speed occurs at the time of applying the load and further the motor runs at a constant speed of 1250 rpm for a load of 2.5 Nm. The estimated load torque waveform is illustrated in Figure 8(d) and is equal is to the applied load. The experimental results are similar to the simulation results and the performance of natural observer is proved experimentally with PI controller.

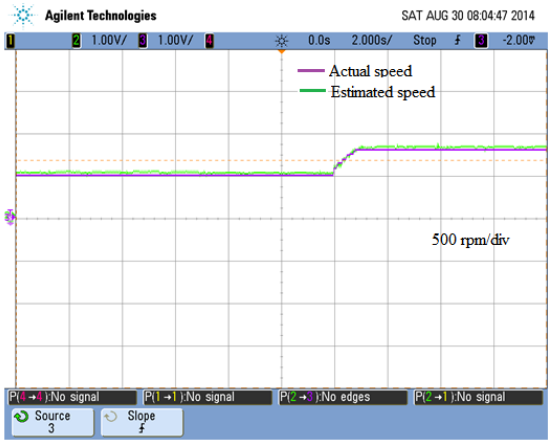

(a) Estimated and actual speed response for a step speed of 1000 rpm and 1250 rpm

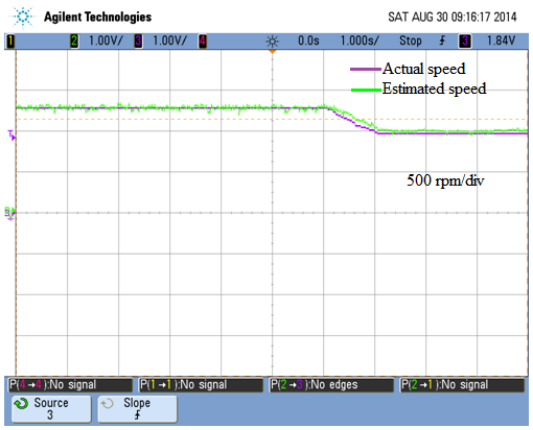

(b) Estimated and actual speed response for a step speed of 1250 rpm and 1000 rpm

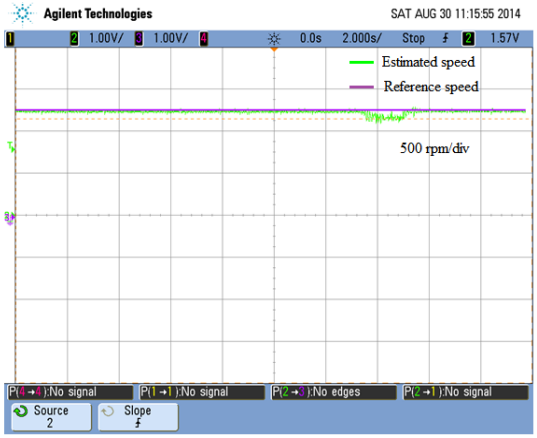

(c) Estimated speed response for a speed command of 1250 rpm and a load of 2.5 Nm

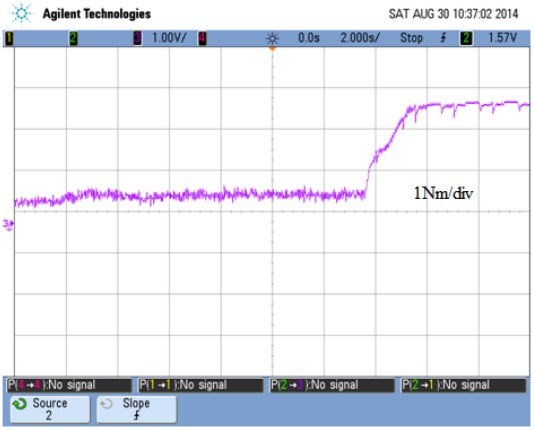

(d) Estimated load torque with 2.5 Nm load for a speed of 1250 rpm

Figure 8 Experimental results for a speed of 1250 rpm with 2.5 Nm load

5. CONCLUSION

The induction motor and the natural observer are modelled in MATLAB with state space and simulations have been carried out for different running conditions. It is concluded that fourth order induction motor model is used and the estimated parameters such as rotor speed and load torque follow the command value. PI controller and fuzzy controllers have been used in the speed control loop to generate the torque reference and their performances have been compared. It is validated that torque ripple in fuzzy controller is less than PI controller. The natural observer is simple and speedy and is a suitable estimator for sensorless vector control of induction motor drive. Mean value of the rotor flux has been maintained constant by employing rotor flux feedback. To validate the simulation, hardware results have been provided for different running conditions.

REFERENCES

[1] Salvatore L, Stasi S, Tarchioni L. A new EKF-based algorithm for flux estimation in induction machines. *IEEE Transactions on Industrial Electronics*. 1993; 40 (5): 496-504.
[2] Kim YR, Seung-Ki Sul, Park MH, Speed sensorless vector control of induction motor using Extended Kalman Filter. *IEEE Transactions on Industry Applications*. 1994; 30(5):1225-1233.
[3] Kim HW, Sul SK. A New motor Speed Estimator Using Kalman Filter in Low-Speed range. *IEEE Transactions on Industry Appications*. 1996; 43 (4):498-504.
[4] Shi KL, Chan TF, Wong YK, Ho SL. Speed estimation of an induction motor drive using an optimized Extended Kalman Filter. *IEEE Transactions on Industrial Electronics*. 2002; 49 (1): 124-133.

[5] Barut M, Bogosyan S, Gokasan M. Speed-sensorless estimation for induction motors using Extended Kalman Filters. *IEEE Transactions on Industrial Electronics*. 2007; 54 (1): 272-280.
[6] Barut M, Bogosyan S, Gokasan M. Experimental evaluation of Braided EKF for sensorless control of induction motors. *IEEE Transactions on Industrial Electronics*. 2008; 55 (2): 620-632.
[7] Kubota H, Matsuse K, Nakano T. *New adaptive flux observer of induction motor for wide speed range motor drives.* 16th IEEE industrial electronics society annual conference, 1990; 921-926.
[8] Kubota H, Matsuse K. Speed sensorless field-oriented control of induction motor with rotor resistance adaptation. *IEEE Transactions on Industry Appications*. 1994; 30 (5): 1219–1224.
[9] Yamada T, Matsuse K, Sasagawa K. *Sensorless control of direct field oriented induction motor operating at high efficiency using adaptive rotor flux observer*. 22nd IEEE international conference on industrial electronics, control and instrumentation, 1996; 1149-1154.
[10] Tsuji M, Umesaki Y, Nakayama R, Izumi K. *A Simplified MRAS based sensorless vector control method of induction motor*. IEEE international conference on power conversion, 2002; 3: 1090-1095.
[11] Bowes SR, Sevinc A, Holliday D. New natural observer applied to speed sensorless DC servo and induction motors. *IEEE Transactions on Industry Appications.* 2004; 51 (5), 1025–1032.
[12] Erenoglu I, Eksin I, Yesil E, Guzelkaya M, *An intelligent fuzzy hybrid fuzzy PID controller*. 20th European Conference on Modelling and Simulation Wolfgang Borutzky, Alessandra Orsoni, Richard Zobel, 2006.
[13] Abdullah I, Al-Odienat, Ayman A, Al-Lawama. The advantages of PID fuzzy controllers over the conventional types. *American Journal of Applied Sciences*, 2008; 6: 653-658.
[14] Subramanyam MV, Prasad PVN, Poornachandra Rao G. Fuzzy logic closed loop control of 5 level MLI driven three phase induction motor. *International Journal of Power Electronics and Drive System* (IJPEDS). 2013: 3 (2): 200-208.
[15] Khobaragade T, Barve A. Enhancement of power system stability using fuzzy logic controller**.** *International Journal of Power Electronics and Drive System* (IJPEDS), 2012: 2 (4): 389-401.
[16] Bose, BK. Modern Power Electronics and AC Drives, Prentice-Hall, Upper Saddle River, New Jersey, 2001.